Noble-metal-free NiFe nanoparticles immobilized on nano $CeZrO_2$ solid solutions for highly efficient hydrogen production from hydrous hydrazine

Hongtao Zou, Qilu Yao, Meiling Huang, Meihua Zhu, Fei Zhang, Zhang-Hui Lu*

Institute of Advanced Materials (IAM), College of Chemistry and Chemical Engineering, Jiangxi Normal University, Nanchang 330022, P.R. China.

E-mail: luzh@jxnu.edu.cn

Synthesis of $Ce_{1-x}Zr_xO_2$ solid solutions

Typically, 1.0 g of Pluronic 123 was dissolved in 10 mL of ethanol with vigorous stirring at 35 °C for 2 h. Then 10 mL quantitative amounts of $Ce(NO_3)_3 \cdot 6H_2O$ and $ZrOCl_2 \cdot 8H_2O$ alcohol solution are dropped slowly into the above solution (total amount of Ce plus Zr is 10 mmol). After being stirred for 4 h, the homogeneous sol was transferred to an oven and underwent solvent evaporation. After aging for 48 h at 40 °C, the gel product were calcined by slowly increasing the temperature from room temperature to 400 °C (1 °C/min ramping rate) and holding at 400 °C for 4 h in muffle furnace to obtain $Ce_{1-x}Zr_xO_2$ solid solutions, where x is the mole ratio of Zr to (Ce + Zr) in the catalysts. For comparison, with different rare earth groups, $La_{0.9}Zr_{0.1}O_2$ and $Nd_{0.9}Zr_{0.1}O_2$ were also prepared by the same method as $Ce_{0.9}Zr_{0.1}O_2$ replacing $Ce(NO_3)_3 \cdot 6H_2O$ with $La(NO_3)_3 \cdot 6H_2O$ and $Nd(NO_3)_3 \cdot 6H_2O$, respectively.

Calculation method for TOF

The turnover frequency (TOF) reported in this work is an apparent TOF value based on the number of (Ni + Fe) atoms in the catalyst, which is calculated from the equation as follows:

$$\mathrm{TOF} = \frac{2\,\mathrm{P}_0 V}{3\,\mathrm{RT} n_{\mathrm{NiFe}} \mathrm{t}}$$

P_0 is the atmospheric pressure (101325 Pa), V is the volume of generated gas (H_2 + N_2) when the conversion reached 50%, R is the universal gas constant (8.3145 $m^3 \cdot Pa \cdot mol^{-1} \cdot K^{-1}$), T is the room temperature (298 K), n_{NiFe} is the total number of moles of (Ni + Fe) atoms in the catalyst and t is the reaction time when the conversion reached 50%.

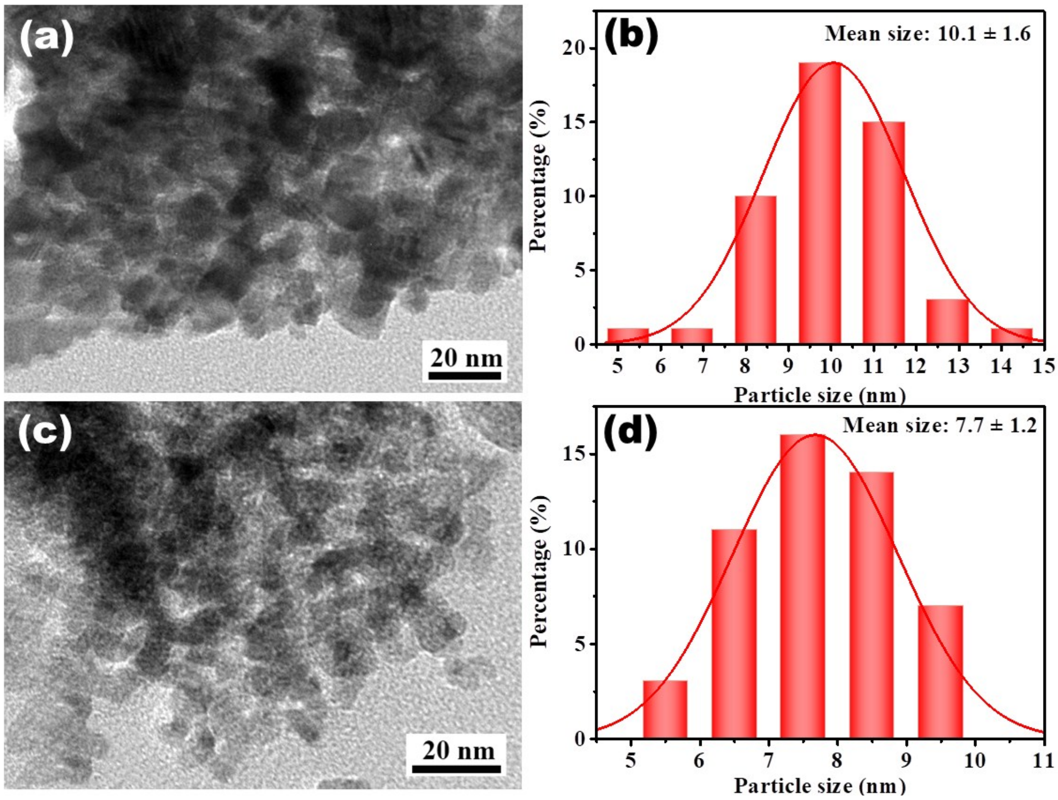

Fig. S1 TEM images and the corresponding particle size distribution of the as-synthesized (a,b) CeO_2 and (c,d) ZrO_2.

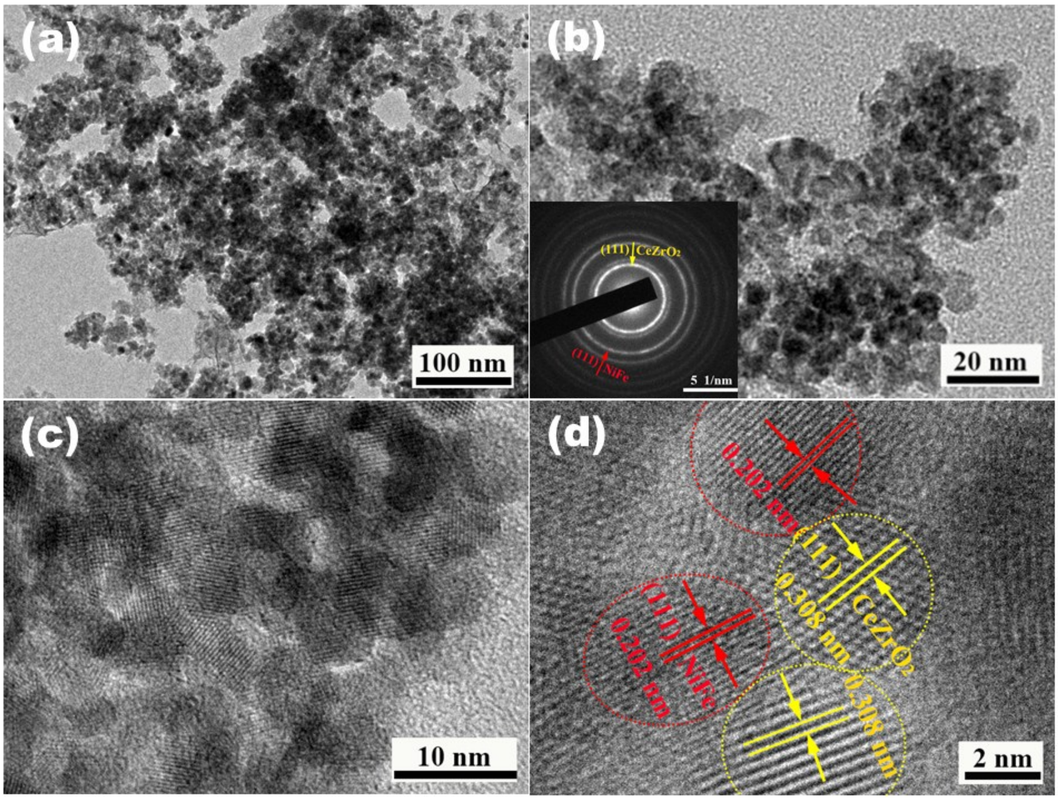

Fig. S2 (a,b) TEM images and (c,d) high-resolution TEM images of the as-synthesized NiFe/$CeZrO_2$ catalyst. The inset of (b) shows the corresponding SAED pattern.

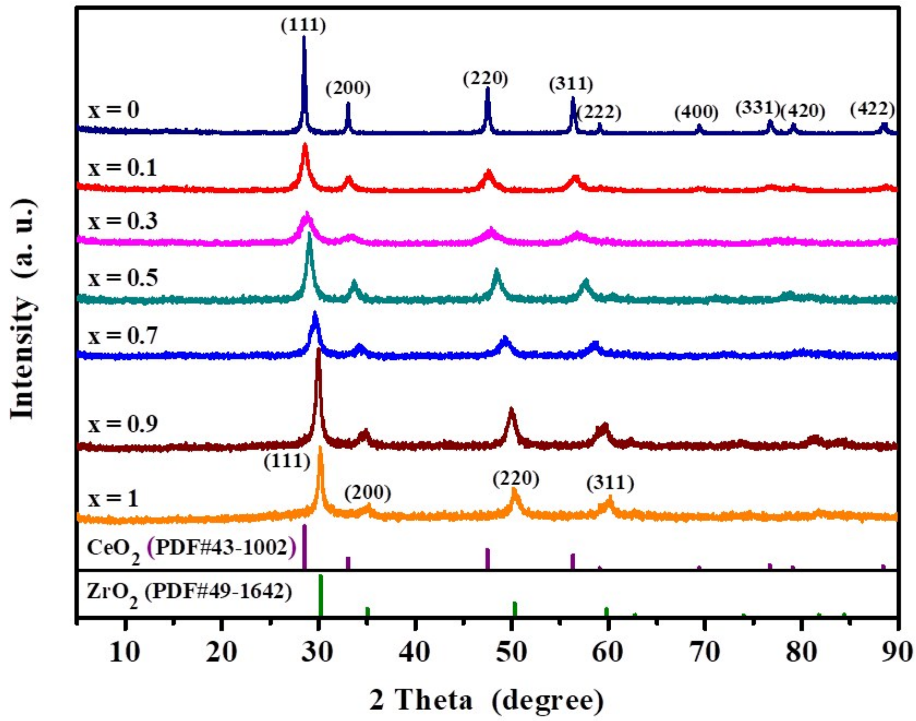

Fig. S3 Powder XRD patterns of the as-synthesized nano $Ce_{1-x}Zr_xO_2$ solid solutions (x = 0, 0.1, 0.3, 0.5, 0.7, 0.9 and 1.0).

The diffraction peaks at 28.52°, 33.08°, 47.52°, 56.40°, 59.08°, 69.40°, 76.70°, 79.12° and 88.38° were assigned to the (111), (200), (220), (311), (222), (400), (331), (420) and (422) crystal facets of CeO_2.

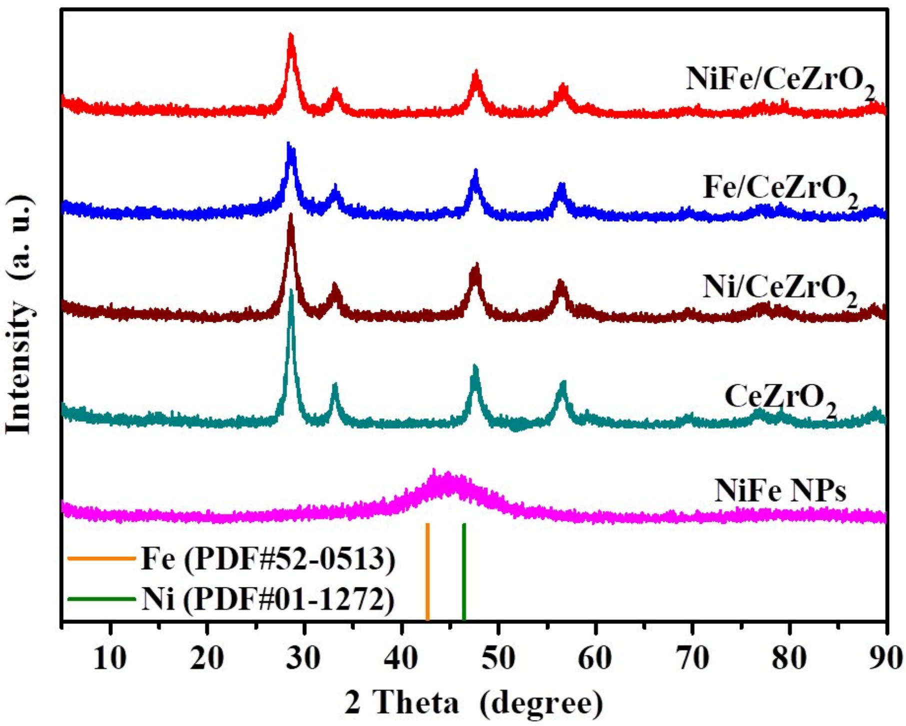

Fig. S4 Powder XRD patterns of the as-synthesized catalysts.

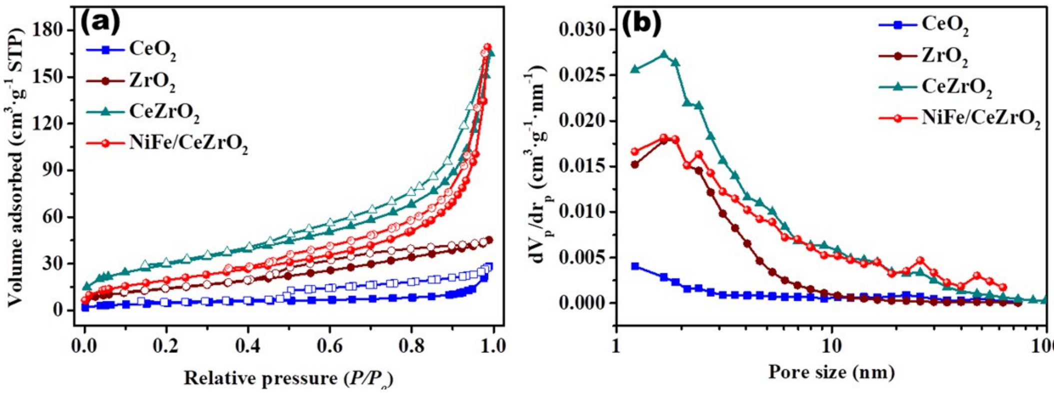

Fig. S5 (a) Nitrogen sorption isotherms and (b) the corresponding pore size distribution curves of CeO_2, ZrO_2, $CeZrO_2$ and $NiFe/CeZrO_2$ catalysts.

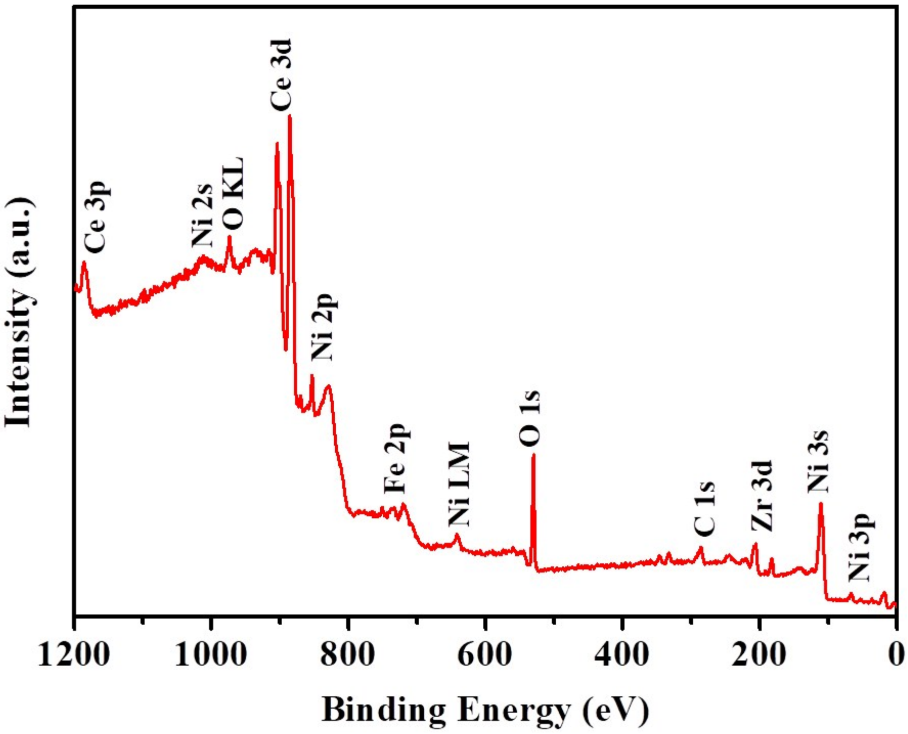

Fig. S6 The survey XPS spectrum of NiFe/$CeZrO_2$ catalyst.

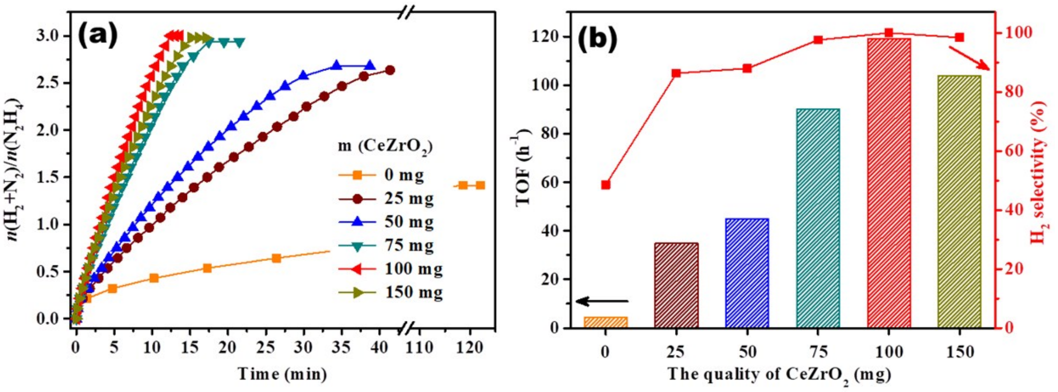

Fig. S7 (a) Time course plots and (b) the corresponding TOF values and H_2 selectivity for H_2 release from N_2H_4 aqueous solution (200 mM, 10 mL) over NiFe/$CeZrO_2$ catalysts with different $CeZrO_2$ contents in the presence of NaOH (2.5 M) at 343 K ($n_{NiFe}/n_{N_2H_4 \cdot H_2O} = 0.1$).

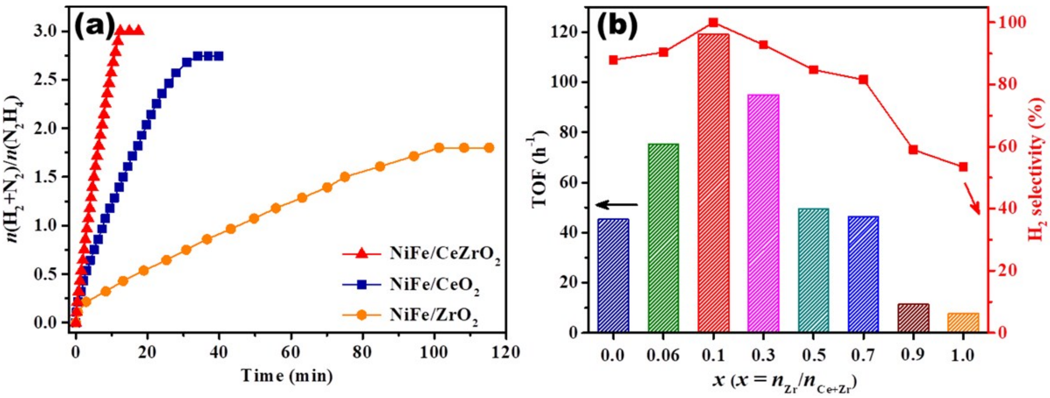

Fig. S8 (a) Time course plots for H_2 release from N_2H_4 aqueous solution (200 mM, 10 mL) over NiFe/$CeZrO_2$, NiFe/CeO_2 and NiFe/ZrO_2 catalysts with NaOH (2.5 M) at 343 K ($n_{NiFe}/n_{N_2H_4\cdot H_2O}$ = 0.1). (b) The TOF values and corresponding H_2 selectivity for dehydrogenation of N_2H_4 aqueous solution over NiFe/$Ce_{1-x}Zr_xO_2$ with different Ce and Zr contents.

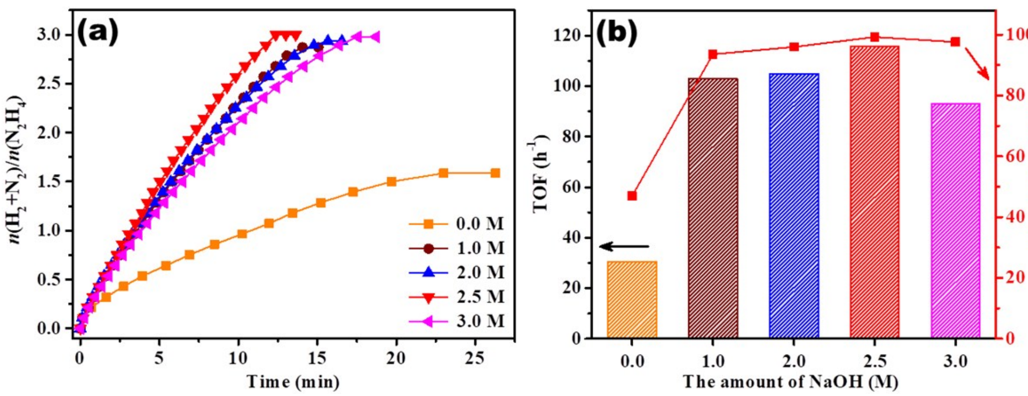

Fig. S9 (a) Time course plots and (b) the corresponding TOF values and H_2 selectivity for H_2 release from N_2H_4 aqueous solution (200 mM, 10 mL) over NiFe/$CeZrO_2$ catalyst with different concentration of NaOH at 343 K (m_{CeZrO_2} = 100 mg, $n_{NiFe}/n_{N_2H_4 \cdot H_2O}$ = 0.1).

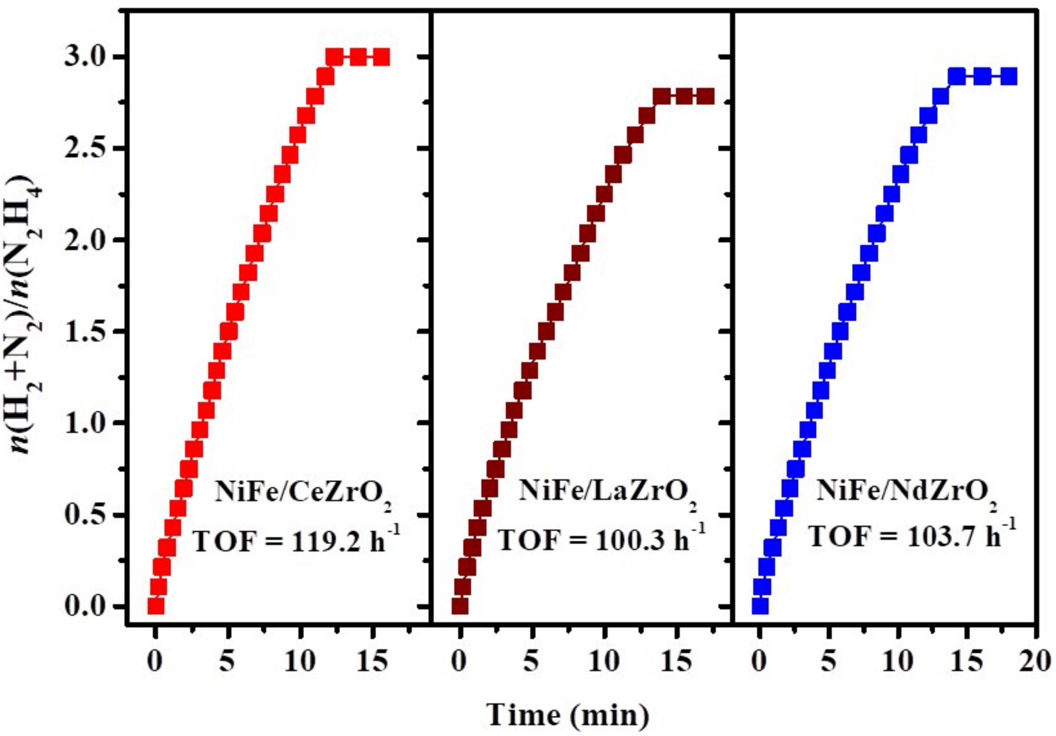

Fig. S10 Time course plots for H_2 release from N_2H_4 aqueous solution (200 mM, 10 mL) over the NiFe/ReZrO$_2$ catalysts (Re = Ce, La, Nd) with NaOH (2.5 M) at 343 K (m_{ReZrO_2} = 100 mg, $n_{NiFe}/n_{N_2H_4 \cdot H_2O}$ = 0.1).

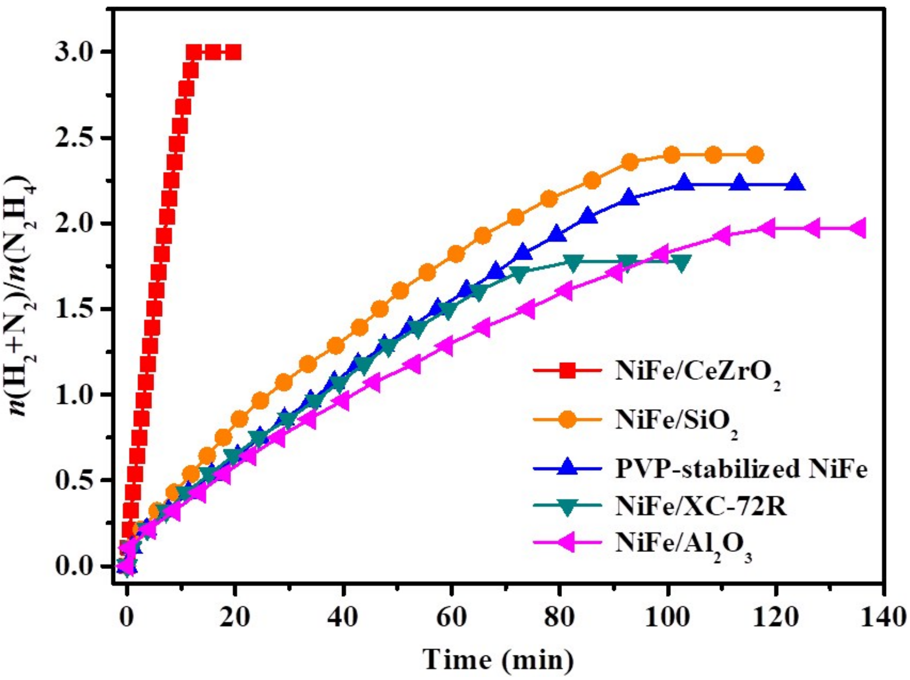

Fig. S11 Time course plots for H_2 release from N_2H_4 aqueous solution (200 mM, 10 mL) over NiFe supported by different supports with NaOH (2.5 M) at 343 K ($n_{NiFe}/n_{N_2H_4 \cdot H_2O} = 0.1$).

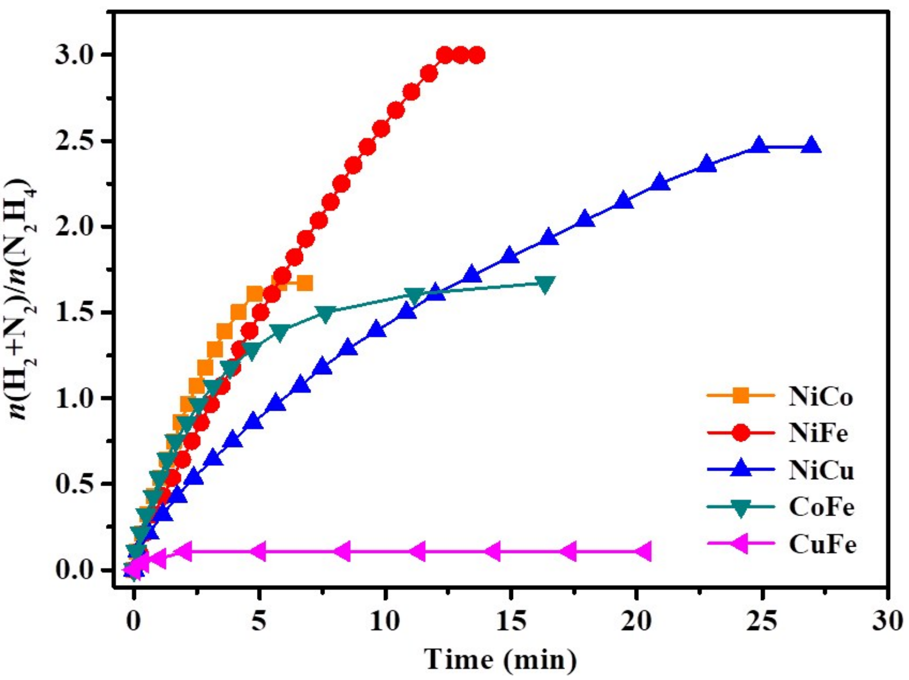

Fig. S12 Time course plots for H_2 release from N_2H_4 aqueous solution (200 mM, 10 mL) over $NiCo/CeZrO_2$, $NiFe/CeZrO_2$, $NiCu/CeZrO_2$, $CoFe/CeZrO_2$ and $CuFe/CeZrO_2$ catalysts with NaOH (2.5 M) at 343 K (m_{CeZrO_2} = 100 mg, $n_{NiFe}/n_{N_2H_4 \cdot H_2O} = 0.1$).

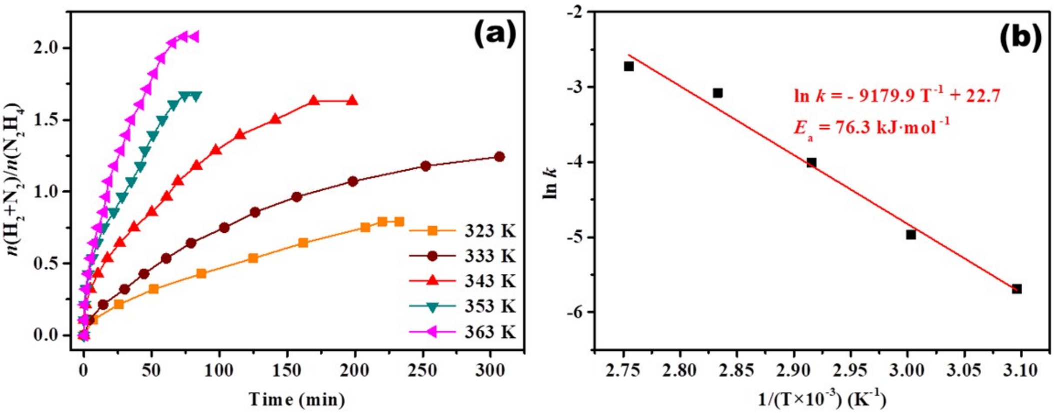

Fig. S13 (a) Time course plots (b) arrhenius plots for H_2 release from N_2H_4 aqueous solution (200 mM, 10 mL) over NiFe NPs with NaOH (2.5 M) at different temperatures ($n_{NiFe}/n_{N_2H_4 \cdot H_2O} = 0.1$).

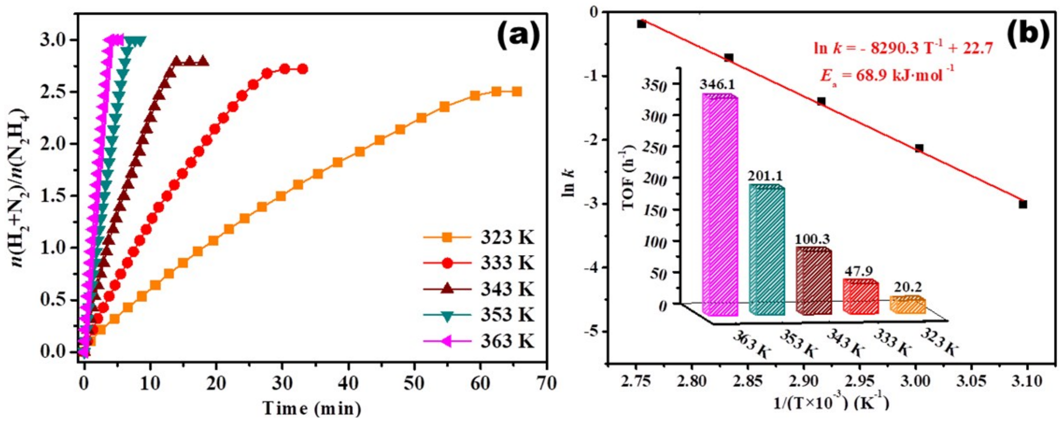

Fig. 14 (a) Time course plots for H_2 release from N_2H_4 aqueous solution (200 mM, 10 mL) over the NiFe/$LaZrO_2$ catalyst with NaOH (2.5 M) at different temperatures. (b) Arrhenius plots and (inset) the corresponding TOF values (m_{LaZrO_2} = 100 mg, $n_{NiFe}/n_{N_2H_4 \cdot H_2O} = 0.1$).

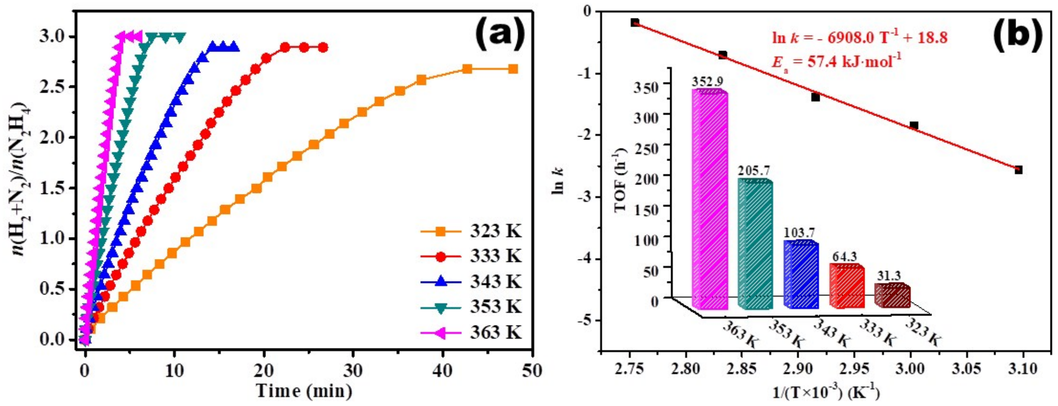

Fig. 15 (a) Time course plots for H_2 release from N_2H_4 aqueous solution (200 mM, 10 mL) over the NiFe/NdZrO$_2$ catalyst with NaOH (2.5 M) at different temperatures. (b) Arrhenius plots and (inset) the corresponding TOF values (m_{NdZrO_2} = 100 mg, $n_{NiFe}/n_{N_2H_4 \cdot H_2O} = 0.1$).

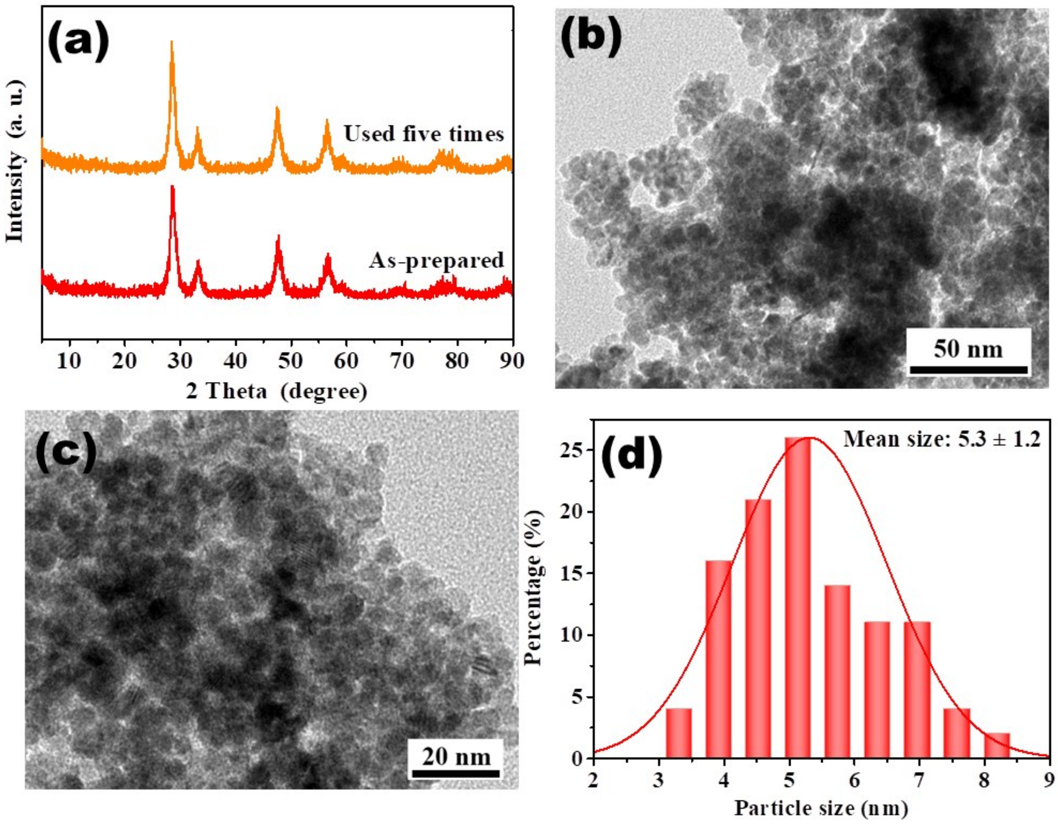

Fig. S16 (a) Powder XRD patterns of the as-synthesized NiFe/$CeZrO_2$ catalysts before and after five times used; (b,c) TEM images of the NiFe/$CeZrO_2$ catalyst used five times and (d) the corresponding particle size distribution.

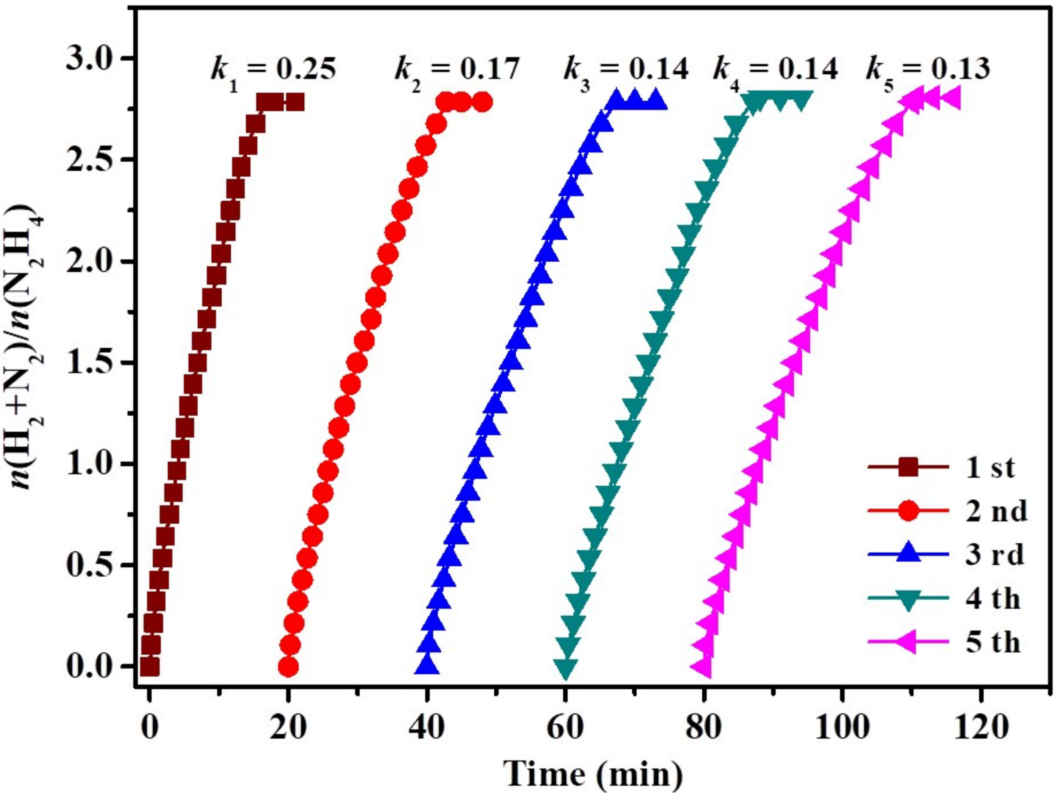

Fig. S17 Stability test for H_2 release from N_2H_4 aqueous solution over the $NiFe/LaZrO_2$ catalyst with NaOH (2.5 M) at 343 K.

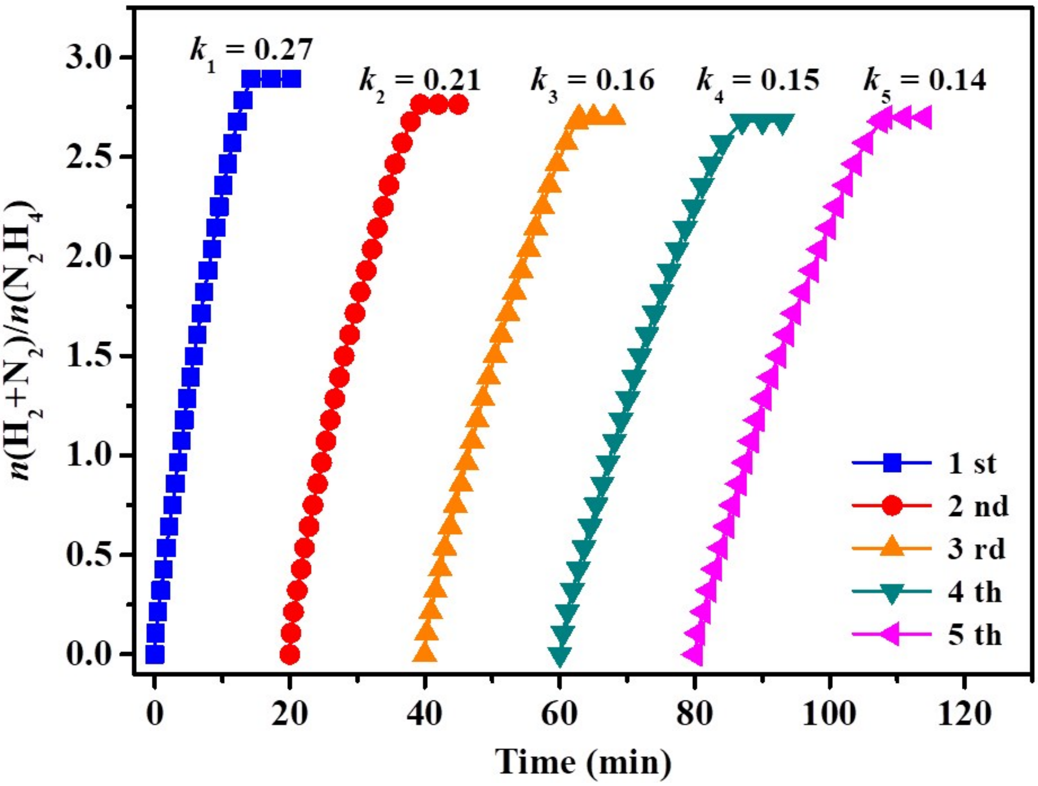

Fig. S18 Stability test for H_2 release from N_2H_4 aqueous solution over the $NiFe/NdZrO_2$ catalyst with NaOH (2.5 M) at 343 K.

Table S1. Catalysts composition determined by inductively coupled plasma atomic emission spectroscopic (ICP-OES).

Catalysts	Ni (wt%)	Fe (wt%)	Ni/Fe (molar ratio)
Fe	-	10.25	-
$Ni_{0.2}Fe_{0.8}$	2.76	9.02	0.23/0.77
$Ni_{0.4}Fe_{0.6}$	4.32	6.83	0.38/0.62
$Ni_{0.6}Fe_{0.4}$	6.96	4.50	0.60/0.40
$Ni_{0.7}Fe_{0.3}$	8.06	3.47	0.69/0.21
$Ni_{0.8}Fe_{0.2}$	9.11	2.41	0.78/0.22
$Ni_{0.9}Fe_{0.1}$	10.08	1.39	0.87/0.13
Ni	11.26	-	-

Table S2. BET surface area, pore volume and pore diameter of different samples.

Samples	BET surface area ($m^2.g^{-1}$)	Pore volume ($cm^3.g^{-1}$)
$CeZrO_2$	108.6	0.2526
$NiFe/CeZrO_2$	74.2	0.2614
ZrO_2	52.2	0.0699
CeO_2	16.9	0.0438

Table S3. Catalytic activities of as-synthesized catalysts toward the dehydrogenation of N_2H_4 in aqueous solution compared to other reported catalysts.

Catalysts	T (K)	NaOH (M)	Selectivity (%)	TOF (h^{-1})	Ref.
NiFe	343	0.5	100	6.3	SI
Ni/Al_2O_3	303	-	93	2.2	S2
$Ni_{0.080}/CeO_2$	303	-	>99	51.6	S3
$Ni_{0.5}Cu_{0.5}$/MCNS	333	0.5	100	21.8	S4
$Ni_{1.5}Fe_{1.0}$-alloy/$(MgO)_{3.5}$	299	-	99	10.9	S5
NiFe/Cu	343	-	100	35.3	S6
$Cu@Fe_5Ni_5$	343	0.1	100	18.2	S7
$Ni_{0.6}Fe_{0.4}Mo$	323	1.8	100	28.8	S8
2D $NiFe/CeO_2$	323	-	99	11.5	S9
Ni_3Fe-$(CeO_x)_{0.15}$/rGO	343	1.0	100	126.2	S10.
NiCo/NiO-CoO_x	298	-	99	11.0	S11
NiMoB-$La(OH)_3$	323	2.0	100	13.3	S12
$NiFe/CeZrO_2$	343	2.5	100	119.2	This work
$NiFe/LaZrO_2$	343	2.5	91	100.3	This work
$NiFe/NdZrO_2$	343	2.5	96	103.7	This work

References

S1 S. K. Singh, A. K. Singh, K. Aranishi and Q. Xu, *J. Am. Chem. Soc.*, 2011, **133**, 19638-19641.

S2 L. He, Y. Q. Huang, A. Q. Wang, X. D. Wang, X. W. Chen, J. Jose Delgado and T. Zhang, *Angew. Chem., Int. Ed.*, 2012, **51**, 6191-6194.

S3 L. He, B. L. Liang, L. Li, X. F. Yang, Y. Q. Huang, A. Q. Wang, X. D. Wang and T. Zhang, *ACS Catal.*, 2015, **5**, 1623-1628.

S4 H. Yen, Y. Seo, S. Kaliaguine and F. Kleitz, *ACS Catal.*, 2015, **5**, 5505-5511.

S5 W. Gao, C.M. Li, H. Chen, M. Wu, S. He, Wei M, D. G. Evans and X. Duan, *Green Chem.*, 2014, **16**, 1560-1568.

S6 K. V. Manukyan, A. Cross, S. Rouvimov, J. Miller, A. S. Mukasyan and E. E. Wolf, *Appl. Catal., A*, 2014, **476**, 47-53.

S7 J. Wang, Y. Li and Y. Zhang, *Adv. Funct. Mater.*, 2014, **24**, 7073-7077.

S8 H. L. Wang, J. M. Yan, S. J. Li, X. W. Zhang and Q. Jiang, *J. Mater. Chem. A*, 2015, **3**, 121-124.

S9 D. D. Wu, M. Wen, C. Gu and Q. S. Wu, *ACS Appl. Mater. Interfaces*, 2017, **9**, 16103-16108.

S10 Y. N. Men, X. Q. Du, G. Z. Cheng and W. Luo, *Int. J. Hydrogen Energy*, 2017, **42**, 27165-27173.

S11 D. D. Wu, M. Wen, X. J. Lin, Q. S. Wu, C. Gu and H. X. Chen, *J. Mater. Chem. A*, 2016, **4**, 6595-6602.

S12 J. J. Zhang, Q. Kang, Z. Q. Yang, H. B. Dai, D. W. Zhuang and P. Wang, *J. Mater. Chem. A*, 2013, **1**, 11623-11628.